Reaction Kinetics, Mechanisms and Catalysis
https://doi.org/10.1007/s11144-024-02677-z

Adsorption study of methylene blue dye removal with activated carbon derived from *Leucaena leucocephala* wastes prepared via H_3PO_4 activation

Nour El Houda Laouar[1] · **Abdelhamid Boukerroui**[1] · **Chafika Meziti**[1,2] · **Sylia Azoug**[1]

Received: 28 April 2024 / Accepted: 23 June 2024

Abstract

This study aims to valorize agricultural waste of *Leucaena leucocephala* pods (LP) as a low-cost precursor for synthesizing high-performance activated carbon (LP-AC) for the removal of methylene blue dye (MB). Phosphoric acid H_3PO_4 was employed as a chemical activator of the LP biomass with a mass ratio of phosphoric acid to the precursor (3/1) before being calcined at 500 °C for 55 min. Box Benken design was investigated to optimize the experimental parameters of initial concentration, adsorbent dose, and pH. Variable optimization indicated that the highest removal efficiency of MB dye, estimated as 99.99%, was noticed at the initial concentration of 300.87 mg L^{-1}, adsorbent dose of 0.049 g, and solution pH of 10.07. Isotherm study revealed that Temkin model shows the best agreement with the experimental data with a correlation coefficient of ($R^2 = 0.990$). The adsorption capacity of MB dye was determined as 584.32 mg g^{-1}. The kinetic study suggested that the pseudo-second-order model is the best-correlated model for data fitting with ($R^2 > 0.997$). The thermodynamic analysis indicated an enthalpy change (ΔH) of − 18.50 kJ/mol, confirming that the adsorption of MB dye onto LP-AC material is an exothermic process. SEM characterization of the surface showed that the LP-AC exhibits a heterogeneous structure. The BET analysis revealed a remarkable surface area of 1367.30 m^2 g^{-1} for the produced carbon, including a blend of mesoporous and microporous structures. Furthermore, complementary analyses including EDS, TGA, and FTIR confirmed the presence of crucial properties, underscoring its potential effectiveness as an adsorbent for removing MB dye.

Keywords *Leucaena leucocephala* pod · Dye removal · Box Benken · Kinetic study · Temkin

Extended author information available on the last page of the article

Published online: 01 July 2024

Introduction

The presence of dyes in water is one of the major causes of water pollution, even at low concentrations, because of their high solubility in water and resistance to bio-degradability [1, 2]. These toxic substances have a detrimental impact on aquatic life, not only because they prevent light from reaching aquatic plants, which hinders the photosynthesis process, but also because they reduce the oxygen ratio in water [3]. For these reasons, the current challenge is discovering an efficient technique to protect the environment from these toxic issues.

In reason of environmental protection, various techniques have been applied in textile industries to eliminate dye from wastewater before being discharged, such as oxidation[4], flocculation [5], membrane filtration [6], biodegradation [7], adsorption [8], electrochemical method [9], photo-oxidation [10]. Adsorption using Carbonaceous materials is supposed to be a better choice for water depollution because of its noticeable surface area, thermal stability, favorable porous structure, high dyes adsorption capacity, and low environmental impact.

The production of a potential activated carbon needs physical and chemical processes that could be costly or consume energy, so endeavors are focused on using economical, renewable, and sustainable sources of the initial precursor [11]. In this pursuit, agricultural wastes are the most commonly applied precursors for activated carbon production, such as rubber leaf [12], sorghum straw[13], *Dacryodes edulis* seeds[14], rice husk [15], soursop seeds [16], *Ficus carica* bast [17], and fig grape leaves [18]. *Leucaena leucocephala* is known for its expeditious growth as an arboreal plant, attaining heights of up to 20 m. This tree is well-known all over the world and grows over an area that is thought to be between 2 and 5 million hectares. A notable feature of this tree is its ability to generate an ample amount of pods on many occasions throughout the year, making it a renewable and accessible resource suitable for exploitation as a precursor in the production of activated carbon [19].

The quality of the carbon produced by the activation process is significantly influenced by the activation conditions that modify the surface proprieties and the adsorption capacity, these conditions include the biomass source, the method of activation, and the chemical activator choice [20]. Chemical activation has been demonstrated as an effective method for preparing potentially activated carbon with highly porous structures. This method provides a significant benefit by requiring lower pyrolysis temperatures and shorter processing periods. Furthermore, it exhibits the potential of creating a high surface area surpassing what can be achieved by the physical activation method [21]. Chemical activation involves the impregnation of the biomass in a chemical activator solution with a specific concentration followed by subjecting the mixture to a thermal treatment. Commonly used activators for chemical activation are H_2SO_4, KOH, NaOH, $Zncl_2$, $KMnO_4$, HNO_3, H_2O_2, H_3PO_4, and K_2CO_3. These activators play a crucial role in enhancing the porosity and adsorption capacity of the produced carbon [22, 23].

Drawing from the previous works on LP biomass, some studies reported the basic activation of LP waste by NaOH where it was applied for the adsorption of dyes and heavy metals [24], while the acidic activation using H_3PO_4 as a chemical activator of LP biomass has not been explored yet. Furthermore, phosphoric acid has been chosen in various studies for its potential to interact with biomass surface, creating high porosity and surface area [25], as demonstrated in previous studies [26–30].

To maximize the efficiency of dye removal, it is essential to optimize the experimental conditions. Response surface methodology (RSM) is a statistical technique that involves the simultaneous variation of the experimental factors to maximize the response, while considering their interaction effects. Furthermore, this technique offers a comprehensive study of how variables influence the response with fewer sets of experiments. In the current study Box Benken design was applied for several reasons, including the efficiency of this model in providing a precise approach to the results and the economic aspect of this model, which offers a reduced set of experiments [31].

The objective of this study is to valorize agricultural wastes in the preparation of ecofriendly activated carbon which demonstrates promising capabilities in textile dye elimination from wastewater. Additionally, the research delves into comprehending the adsorption behavior through isotherm, kinetic, and thermodynamic study, besides the physicochemical characterizations (FTIR, SEM–EDS, TGA, BET, pH_{pzc}) that enhance the identification of the various interactions that occur on the activated carbon structure.

Materials and methods

Preparation of the activated carbon (LP-AC)

Following the washing and drying steps, LP pods was further processed through a grinder to achieve a particle size of 250 µm. The activated carbon was prepared by the impregnation of the biomass in phosphoric acid with concentration of 98% (w/v) and predetermined mass ratio of (1/3), (biomass/H_3PO_4), the mixture was stirred for 4 h to ensure the homogenization of the slurry, then dried in an oven for 24 h at 100 °C. After that, the sample was subjected to pyrolysis in a muffle furnace at 500 °C for 55 min. The carbonized sample was washed abundantly with hot distilled water until the neutralization of the filtrate. Finally, the produced activated carbon was dried at 80 °C, crushed, and sieved to a particle size $<$ 80 µm and kept in an airtight container for further use.

Reagents and apparatus

This study targets methylene blue molecules ($C_{16}H_{18}ClN_3S_3.H_2O$) with a molecular weight of 319.86 g mol^{-1}. Phosphoric acid H_3PO_4, sodium hydroxide NaOH, and hydrochloric acid HCl were acquired from Sigma Aldrich company. The residual concentration of methylene blue was determined using a UV–Visible spectrophotometer type (GENESYS 10SUV-VIS). pH measurements were conducted using pH meter type (OHAUS, STARTER 3100). Design Expert software 13 was used as an analytical tool in the response surface methodology study.

Characterization of the adsorbent

Carbon porosity and surface area were determined using adsorption–desorption isotherms of N_2 at 77 K with relative pressure range $0 < P/P° < 1$ using outgases of 8 h, using Autosorb 1C (Quantachrome) machine. The BET (Brunauer–Emmett–Teller) method was employed to estimate the surface area (S_{BET}) of the prepared activated carbon. Surface functional groups were qualitatively determined using Fourier transform infrared spectroscopy (FTIR) at wave light ranging from 400 to 4000 cm^{-1}, using (Nicolet IS5) instrument. The hydraulic pump was used to produce pellets after mixing 2 mg of the sample with 80 mg of KBr. The surface morphology of the raw LP and LP-AC materials was identified through SEM analysis, applying magnification of ×2500 with a Quanta FEI 250 apparatus. Elemental composition analysis of both raw and activated carbon was determined using EDS analysis. Thermal behavior of LP material was characterized using (TGA/DSC) (thermal gravimetric analysis/differential scanning calorimeter) from room temperature 20 °C up to 600 °C using sta 449F3 jupiter (Netzsch) apparatus.

Adsorption experiment using Box Benken design

Box Benken design was used to determine the optimal conditions for maximizing MB removal using activated carbon within three independent variables and three levels. To create a Box Benken matrix, a series of primary tests is essential to determine the parameters that strongly affect the MB adsorption on the LP-AC material. The independent variables are codded as A: initial concentration, B: initial pH, and C: adsorbent mass. Variables range limits are coded as − 1 for low level and + 1 for high level, while 0 for the central points as summarized in the Table 1. During the adsorption experiment, a mass of adsorbent was added to 50 mL of MB solution and then mixed for 2 h at a shaking speed of 300 rpm. Subsequently, the solid separation was performed using a 0.4 µm filter, and the residual concentration of MB dye was measured at ($\lambda_{max} = 664$ nm). pH solution was adjusted using 0.01 M of HCl and NaOH solutions. Removal efficiency (R %) of dye and the adsorbed amount at the equilibrium q_e (mg g^{-1}) was determined using Eqs. 1 and 2:

Table 1 codded levels of the input variables

Factors	Unit	Codded levels		
		− 1	0	+1
Dye concentration (A)	mg L^{-1}	300	500	700
Initial pH (B)	–	2	7	12
Adsorbent mass (C)	g	0.01	0.03	0.05

$$R\% = \frac{\left(C_0 - C_e\right)}{C_0} \times 100 \tag{1}$$

$$q_e = \frac{\left(C_0 - C_e\right) \times V}{W} \tag{2}$$

Here C_o and C_e (mg L^{-1}) are starting and equilibrium concentrations of MB, V, and W are the solution volume (L) and the adsorbent mass (g). The statistical study of the model was performed using Design Expert (13.0, Stat-Ease, USA).

The mathematical model at the end of the design, which predicts the removal efficiency of MB dye, can be constructed using the following equation:

$$R = \beta_0 + \sum_{i=1}^{K} \beta_i X_i + \sum_{i=1}^{K} \sum_{i=1}^{K} \beta_{ij} X_i X_j + \sum_{i=1}^{K} \beta_{ii} X_i^2 \tag{3}$$

Here R is the output (MB removal efficiency), β_0 is a constant coefficient, β_i, $\beta_{ii,}$ and β_{ij} are regression coefficients of linear interaction, quadratic effect, and linear interaction of variable. X_i, X_j are experimental variables [32, 33].

Isotherm study

Isotherm models mainly explain the interfacial phenomena between the adsorbent and the adsorbate molecules. Various models such as Langmuir, Freundlich and Temkin are used to describe the adsorption behavior under equilibrium conditions. The Langmuir isotherm suggests that the adsorbent sites are covered by a monolayer of the adsorbate molecules occupying uniform sites. The nonlinear form of Langmuir is expressed as [34]:

$$q_e = \frac{\mathrm{q_m K_L C_e}}{1 + \mathrm{K_L C_e}} \tag{4}$$

Here q_m (mg g^{-1}), K_L (L mg^{-1}), and C_e (mg L^{-1}) are the dye maximum adsorption capacity, Langmuir constant, dye concentration at the equilibrium. Adsorption feasibility can be determined using Langmuir dimensionless constant as follows Eq. 5:

$$\mathrm{R}_L = \frac{1}{1 + \mathrm{K_L C_0}} \tag{5}$$

Depending on the R_L values, the adsorption equilibrium can be unfavorable ($R_L > 1$), linear ($R_L = 1$), favorable ($0 < R_L < 1$), or irreversible ($R_L = 0$) [35].

The Freundlich isotherm is employed to describe the adsorption phenomenon on a heterogeneous adsorbent surface, allowing for the formation of multiple layers of solute molecules on the adsorbent surface. The Freundlich non-linear equation can be illustrated as follows [36]:

$$q_e = K_f C_e^{\frac{1}{n}} \tag{6}$$

Here K_f ((mg g^{-1}) (L mg^{-1})$^{1/n}$), C_e (mg g^{-1}), and n are the Freundlich equilibrium constant, equilibrium concentration, and heterogeneity constant respectively.

Temkin isotherm assumes that the heat of the adsorption changes linearly with the surface coverage of the adsorbent molecules. The nonlinear Temkin equation is expressed as:

$$q_e = \frac{RT}{b_T} \ln \left(K_T C_e \right) \tag{7}$$

Here b_T (J mol^{-1}) is the heat adsorption constant, K_T (L mg^{-1}) is the Temkin constant at the equilibrium, T is the temperature in kelvin, R gas constant (8.314 J mol^{-1} K^{-1}) [37].

Results and discussion

Adsorbent characterization

Zero charge point

The adsorbent performance depends on the interactions formed between its surface charge and the charge of the target molecules. Notably, the adsorbent surface could be basic, acidic, or neutral which influences the adsorption efficiency. Fig. S1 (Online Resource 1) represented the zero charge point of the activated carbon determined following the salt addition method as expressed by Manna et al. [38]. It can be seen that the carbon produced has an acidic surface, as indicated by the zero charge point of 2.3. Above this point, the LP-AC surface shows a negative charge, which is favorable for creating electrostatic interactions with positive MB molecules [39].

Textural characteristics of the activated carbon

Nitrogen adsorption–desorption isotherm model was used to study the porosity and texture properties of the activated carbon. According to the IUPAC classification, the observed curve shape in Fig. 1a is of type IV, characterized by a narrow hysteresis loop of type H4 at $0.4 < P/P0 < 1$, indicating the presence of both microporous and mesoporous structure, which is confirmed by the Barrett–Joyner–Halenda (BJH) pore distribution Fig. 1b, where it can be seen that the most of pores sizes are ranging between 1.55 and 9.75 nm, corresponding to micropores with diameters < 2 nm, and mesopores with diameters from 2 to 50 nm [40]. Table 2 shows that the LP-AC exhibits a high BET surface area of 1367.30 m^2 g^{-1} with a significant mesoporous area of 803.95 m^2 g^{-1} which enhance the MB adsorption.

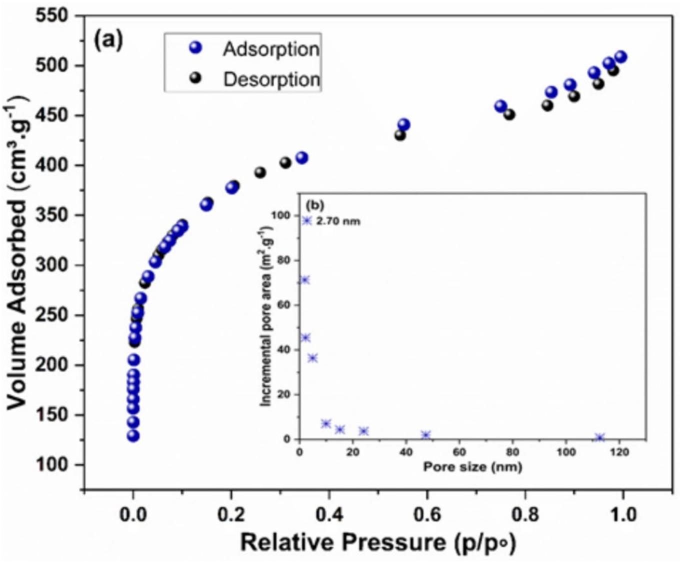

Fig. 1 N2 adsorption–desorption isotherm (**a**), and pore size distribution (**b**) of LP-AC

Table 2 Textural properties of LP-AC

S_{BET} ($m^2\ g^{-1}$)	S_{meso} ($m^2\ g^{-1}$)	S_{mic} ($m^2\ g^{-1}$)	V_t ($cm^3\ g^{-1}$)	V_{mic} ($cm^3\ g^{-1}$)	V_{meso} ($cm^3\ g^{-1}$)	Dp (nm)
1367.30	803.95	563.35	0.78	0.23	0.55	2.30

Dp average pore diameter

FTIR analysis

FTIR analysis was applied to identify the surface functional groups on LP activated carbon as presented in Fig. 2. The broad peak at 3383 cm^{-1} could be attributed to the presence of hydroxyl groups OH originating from alcohol, carboxyl, and phenol, or may occur due to water adsorption. The peak at 1578 cm^{-1} can be associated with the presence of a C=C bond, indicating that the LP-AC may contain aromatic rings [41]. It could be noteced that the intensity of methyle C–H_3 peak at 1311 cm^{-1} is more intense after MB adsorption, besides, the appearance of a new peak at 1319 cm^{-1} which could be due to the formation of electrostatic interactions with MB molecules [42]. Peak at 1211 attributed to the C–O vibration [43]. The peak at 1075 cm^{-1} may refer to the symitric and asymitric vibration of P–O–C and P–O respectively [44, 45]. The appearance of small peaks at around 885–800 cm^{-1} after MB adsorption refers to the =C–H Alkene bonds of the benzen ring [46, 47].

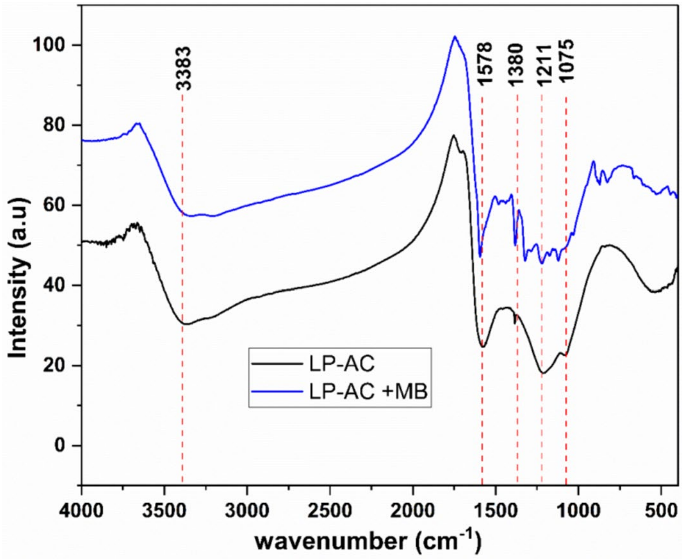

Fig. 2 FTIR analysis of LP-AC before and after MB adsorption

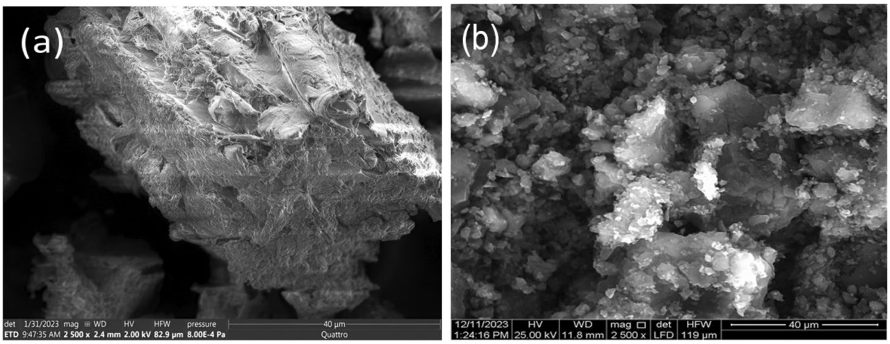

Fig. 3 SEM image for raw LP at ×2500 (**a**), and activated carbon at ×2500 (**b**)

SEM analysis

The effect of the chemical activation on the surface morphology of the activated carbon was determined using SEM analysis as presented in Fig. 3. It is observable that the LP precursor in Fig. 3a is characterized by a wavy, non-porous surface with the presence of wrinkles, which may explain their restricted surface area. while, the produced activated carbon Fig. 3b represents a rough, cracked, and extremely heterogeneous surface that includes various forms of cavities and pits that allow the adsorption of different sizes of solute molecules. Pore formation could be attributed to the reaction of the phosphoric acid with the raw LP during the activation process which leads to the emission of volatile compounds [29, 48, 49]. After MB adsorption

Fig. S2 (Online Resource 1), the surface of LP-AC becomes smoother and denser confirming that the LP-AC surface is covered by MB molecules. However, there are no significant changes in the overall structure of LP-AC.

EDS analysis Fig. S3a and b (Online Resource 1) indicated that the carbon content increases from 52.28 to 80.70% in raw and activated carbon respectively. That could be attributed to the vaporization of volatile substances during the activation process, resulting in a material that has a higher concentration of carbon. This affirms the efficiency of the activation process in carbon production using phosphoric acid. Furthermore, the produced carbon is rich with oxygen and phosphor which is in consistent with the FTIR analysis.

Thermal gravimetric analysis of LP-AC

Thermal gravimetric analysis TGA and differential scanning calorimeter DSC of raw precursor represented in Fig. 4 indicated that LP degradation occurs in three main sections. At the first stage, a small weight loss of 7.62% was observed at temperature of (50–150 °C) because of the volatile matter and water evaporation. At the second stage, a notable mass loss of 46.11% was observed within the temperature range of (200–350 °C). This aligns with earlier studies which suggests that cellulose, hemicellulose, and lignin decompose within the temperature range of (265–310 °C) [50]. At this stage an intense pic of exothermic reaction is observed at 300 °C. The third stage of mass loss corresponds to the degradation of the rest of lignin molecules at temperature range of (350–500 °C) with a mass loss of 32.39%. At temperatures beyond 500 °C, there is no longer any loss of mass, suggesting that this temperature is the most favorable for the production of activated carbon.

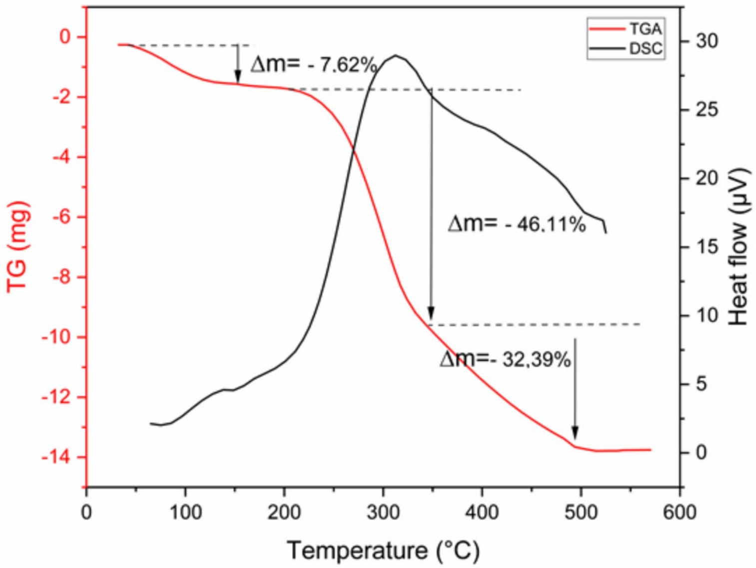

Fig. 4 TGA/DSC analysis of raw LP material

Model fitting and statistical analysis

To evaluate the influence of the experimental variables on the removal efficacy of MB using Lp-activated carbon, a Box–Benken matrix including 17 batch trials was undertaken. During these trials, three variables were manipulated, each with three different levels. The values of MB removal efficiency % are tabulated in Table 3. Notably, the experimental results indicated that the maximum removal efficiency of 99.42% is highlighted in the experiment run 17, under the following conditions: dye concentration of 300 mg L^{-1}, pH solution of 7, and an adsorbent dose of 0.05 g.

The Analysis of variance (ANOVA) was carried out to assess the significance of variables variation on the response at a confidence level of 95%. The validation of model adequacy relies heavily on the model's P and F values, where a small p value (<0.05) and large F value (>0.05) are required for the model significance [51]. The ANOVA results summarized in Table 4 indicated that with p-value <0.0001 and F value of 71.15, the quadratic model chosen is significant for the results fitting. Moreover, the model exhibited a non-significant lack of fit as indicated by a p-value of 0.5948 confirming the suitability and the adequacy of the model.

In addition, an essential set of parameters is required to assess the significance of the model, including the correlation coefficient $R^2=0.9892$, which presents a high value close to 1, suggesting that only 1.08% of the variation remains unexplained by the model [33]. High values were also observed for the adjusted $R^2=0.9753$ and the predicted $R^2=0.9289$, the difference between these two parameters should be less than 0.2 to revealed a good model fit.

Table 3 Box Benken matrix of the tree variables

Run	A: [MB] (mg L^{-1})	B: pH	C: Adsorbent mass (g)	MB removal %
1	500	2	0.01	24.5
2	500	12	0.05	98.41
3	500	7	0.03	63.58
4	500	12	0.01	87.67
5	700	7	0.01	32.53
6	500	2	0.05	86.98
7	700	12	0.03	98.87
8	300	7	0.01	40.52
9	300	2	0.03	81.22
10	500	7	0.03	60.63
11	500	7	0.03	59.87
12	700	2	0.03	43.05
13	300	12	0.03	99.01
14	500	7	0.03	68.69
15	500	7	0.03	68.01
16	700	7	0.05	62.15
17	300	7	0.05	99.42

Table 4 ANOVA test

Source	Sum of squares	df	Mean Square	F-value	p-value	Remark
Model	9327.70	9	1036.41	71.15	< 0.0001	*
A-initial concentration	872.99	1	872.99	59.93	0.0001	*
B-pH	2745.78	1	2745.78	188.50	< 0.0001	*
C-Adsorbent mass	3269.98	1	3269.98	224.48	< 0.0001	*
AB	361.57	1	361.57	24.82	0.0016	*
AC	214.33	1	214.33	14.71	0.0064	*
BC	669.26	1	669.26	45.94	0.0003	*
A^2	0.4400	1	0.4400	0.0302	0.8669	–
B^2	1085.76	1	1085.76	74.54	< 0.0001	*
C^2	142.83	1	142.83	9.81	0.0166	*
Residual	101.97	7	14.57			
Lack of fit	35.42	3	11.81	0.7097	0.5948	–
Pure error	66.54	4	16.64			
Cor total	9429.67	16				

$R^2 = 0.9892$, R^2 Adjusted = 0.9753, R^2 Predicted = 0.9289, * significant, – not significant

The prediction of the removal efficiency of MB dye using LP-AC is represented by a second-degree polynomial Eq. 8. According to the statistical study of the variables, terms with p-values less than 0.05 are important and play an essential role in the model. In this context, A, B, C, AB, AC, BC, B^2, and C^2 are found to be significant contributors. However, A^2 is not significant in this model.

$$R\% = +64.16 - 10.45A + 18.53B + 20.22C + 9.51AB - 7.32AC - 12.94BC + 0.323A^2 + 16.06B^2 - 5.82C^2 \quad (8)$$

To assess the model applicability, the distribution of the model predicted data vs actual data points is illustrated in Fig. S4 (Online Resource 1). It is evident that both results are close, with a uniform distribution that forms a straight line. This could be an emphasis on the accuracy of the model in predicting results [52].

Surface response analysis

Adsorption of MB dyes on LP-AC is influenced by various experimental parameters, including initial dye concentration, solution pH, and Adsorbent dose. These parameters can enhance or impede the removal efficiency of dye. To better understand the interaction effect of parameters on the response, 3D surface response plots were investigated. Fig. 5a shows the interaction effect of the adsorbent dose and pH while holding dye concentration constante at the central point of 500 mg L^{-1}. It could be seen that pH variation has a positive effect on the response where increasing the pH values from 2 to 12 increases removal efficiency from 24 to 86%. That could be a result of the negative charge exhibited by the adsorbent at

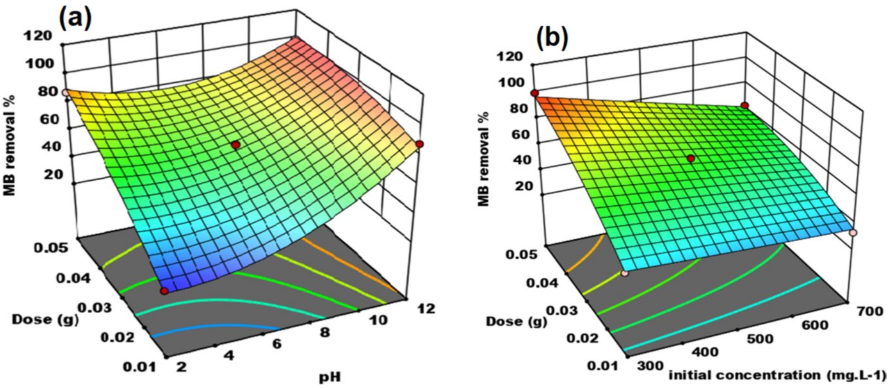

Fig. 5 3D plot of factors interactions, adsorbent dose and pH (**a**), adsorbent dose and initial concentration (**b**) (at V = 50 mL, stirring = 300 rpm, T = 28 °C)

pH values higher than the (pH_{zpc} = 2.3) which is favorite for dropping positive MB molecules [53].

Fig. 5b suggests that increasing the adsorbent dose from 0.01 to 0.05 g, improves the MB uptake, which could be a result of the availability of a large number of vacant sites offered by the adsorbent addition [55].

However, the initial dye concentration has a negative effect on the adsorption performance Fig. S5 (Online Resource 1). As it increases from 300 to 700 mg L^{-1}, the removal efficiency decreases from 81 to 43%, which could be explained by the large number of MB molecules at high concentration against the limited active sites of the adsorbent [54].

Optimization of experimental parameters using the desirability function

The desirability function (DF) plays an essential role in optimizing the experimental parameters for maximizing the removal efficiency of MB dye. The scenario chosen for this optimization was based on keeping all variable values within range while maximizing the response. According to the ramp function graph Fig. S6 (Online Resource 1), achieving a removal efficiency of 100.18% with a desirability of 1% corresponds to setting the value of the parameters at an initial dose of 0.049 g, dye concentration of 300.87 mg L^{-1}, pH of 10.07. For the validation of the scenario Table 5 represents the predicted and the experimental values of the responses. It

Table 5 Relative error for the model validation

Optimal values of the adsorption		Predicted response %	Experimental validation %	Error %
[MB]	300.87 mg L^{-1}	100.18	99.99	0.19
pH	10.07			
Adsorbent dose	0.049 g			

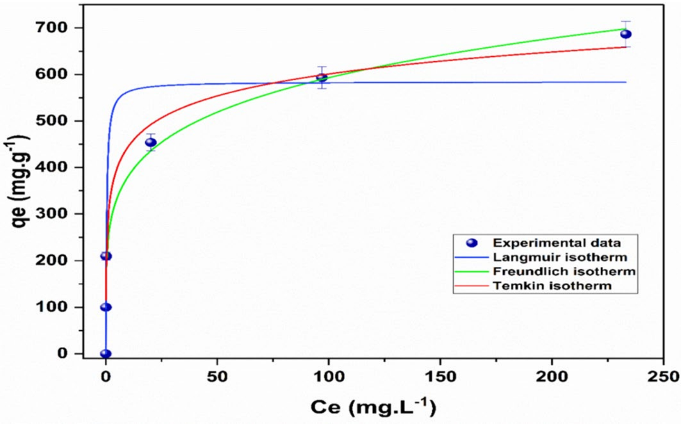

Fig. 6 Isotherm models of Langmuir, Frendlich, and Temkin (at adsorbent mass = 0.049 g, V = 50 mL, t = 2 h, stirring = 300 rpm, T = 28 °C, pH 10.07)

Table 6 Isotherm parameters of Langmuir, Freundlich, and Temkin

Adsorption isotherm	Parameters	Values ± SE
Langmuir	q_m (mg g^{-1})	584.32 ± 46.81
	K_L (L mg^{-1})	2.61 ± 1.37
	R^2	0.934
	R_L	3.82×10^{-4} ± 1.37
Freundlich	K_f ((mg g^{-1}) (L $mg^{-1})^{1/n}$)	244.117 ± 23.29
	1/n	0.192 ± 0.02
	R^2	0.984
Temkin	K_T (L mg^{-1})	68.327 ± 28.20
	b_T (J mol^{-1})	37.008 ± 4.106
	R^2	0.990

could be noticed that the experimental validation of these conditions shows a removal efficiency of 99.99%, this value is so close to the value predicted by the model. The error calculated using Eq. 9 is estimated as 0.19% this small value is acceptable for the validation of the model prediction. The experiments were repeated at least two times.

$$Error\% = \left|\frac{Experimentale\ value - Predicted\ value}{Exprimentale\ value}\right| * 100 \tag{9}$$

Isotherm study

The isotherm study was conducted using the nonlinear forms of the most commonly employed Langmuir, Freundlich, and Temkin isotherms [56]. Fig. 6 shows the variation of the adsorbed amount as a function of the equilibrium dye concentration varied in the range (100 to 1000 mg L^{-1}), the rest of the experimental conditions were fixed at the optimal values previously determined in the RSM study. The equilibrium parameters of the model fitting are calculated in Table 6.

To evaluate the best fitted model, the isotherms were compared using R^2 values. Both Temkin and Freundlich have higher coefficients than the Langmuir isotherm. Temkin isotherm shows the best agreement with the experimental data with $R^2=0.980$ indicating the heterogeneity in the adsorbent site energy. The positive value obtained for the adsorption heat calculated from the Temkin isotherm ($b_T>1$) revealed that the adsorption process is exothermic [57, 58]. Langmuir isotherm represents a maximum adsorption capacity of $q_m=584.32$ mg g^{-1}. The obtained adsorption capacity indicated that the produced activated carbon shows a high performance compared to those obtained from different activated carbons for MB removal derived from Garcinia mangostana $q_m=163.6$ mg g^{-1} [27], pistachio shells $q_m=129$ mg g^{-1} [59], corn cob residue $q_m=183.3$ mg g^{-1} [60], *Calicotome villosa* $q_m=169.78$ mg g^{-1} [61]. Furthermore, the R_L value less than the unit indicates a favorable adsorption process. Additionally, Freundlich constant $1/n<1$ indicated that MB adsorption on LP activated carbon is a favorable process.

Kinetic study

The kinetic mechanism of the adsorption of MB dye on activated carbon was investigated using the two basic models of Pseudo first order and Pseudo second order using the following equations:

Pseudo first order

$$q_t = q_e\left(1 - e^{-K_1 \cdot t}\right) \tag{10}$$

Pseudo second order

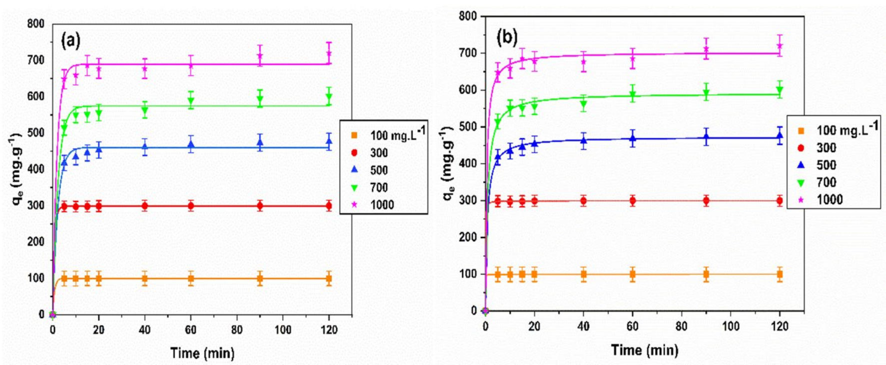

Fig. 7 kinetic plots of pseudo first order (**a**), and pseudo second order (**b**) (at adsorbent mass = 0.049 g, V = 50 mL, t = 2 h, stirring = 300 rpm, T = 28 °C, pH 10.07)

Table 7 Kinetic parameters of MB adsorption on LP-AC

C_0 (mg L^{-1})	Pseudo first order			Pseudo second order		
	K_1 (min^{-1})	R^2	Standard error	K_2 (g mg^{-1} min^{-1})	R^2	Standard error
100	1.265	0.999	0.003	0.725	1.000	0.0010
300	1.214	0.999	0.034	0.095	0.999	0.0012
500	0.454	0.993	0.009	0.002	0.999	0.0056
700	0.436	0.990	0.004	0.002	0.997	0.0021
1000	0.546	0.995	0.008	0.003	0.998	0.0002

$$q_t = \left(K_2 q_e^2 \cdot t\right) / \left(1 + K_2 q_e \cdot t\right) \tag{11}$$

Here q_e and q_t are the dye amount at equilibrium and instant t, K_1 (L min^{-1}) is the pseudo first order constant, K_2 (g mg^{-1} min^{-1}) is the pseudo-second order constant respectively.

Non-linear fitting of the adsorbed amount in function of initial dye concentration is illustrated in Fig. 7. It appears that the equilibrium is achieved in the first 5 min for low concentrations, whereas it necessitates a longer time for high concentrations, typically around 20 min. kinetic parameters derived from the non-linear fitting are illustrated in Table 7. Upon comparing the correlation coefficients, it is evident that the PSO model shows significantly higher values with $R^2 > 0.997$, in contrast to the PFO model with $R^2 > 0.990$.

Furthermore, the normalized standard deviation of the adsorbed amount Δq% calculated from Eq. 12 indicated that the PSO model is in better agreement with the experimental data, as indicated by the lowest value of Δq = 0.636% compared to the high value obtained from the PFO model Δq = 1.71%, suggesting that chemisorption interactions govern the kinetic rate of the process [62]. These results are in line with those found in a previous study on the adsorption of MB dye on phosphoric-activated carbon [63–65].

$$\Delta q\% = 100 \times \frac{\sqrt{\sum_{i=1}^{n}\left(\frac{q_{eexp} - q_{ecal}}{q_{ecal}}\right)^2}}{n - 1} \tag{12}$$

Thermodynamic study

To investigate the effect of temperature on the adsorption of MB dye on the activated carbon, the temperature effect was carried out in a range of (303, 313, 323, and 333 K) using dye concentration of 300 mg L^{-1}, adsorbent mass of 0.045 g, pH of 10.07. Thermodynamic parameters of Gibbs free energy ΔG, enthalpy ΔH, and entropy ΔS were calculated using the following equations:

$$K_d = \frac{q_e}{c_e} \tag{13}$$

$$\Delta G^{\circ} = -RT \ln K_d \tag{14}$$

$$\ln K_d = \frac{\Delta S^{\circ}}{R} - \frac{\Delta H^{\circ}}{RT} \tag{15}$$

Here q_e is the dye adsorbed amount at the equilibrium, Ce is the equilibrium concentration, K_d (L g^{-1}) is the equilibrium constant, R is the molar gas constant (8.314 J mol^{-1} K^{-1}) and T is the temperature in kelvin.

The thermodynamic parameters summarized in Table 8 showed negative values for both enthalpy ΔH and entropy ΔS, indicating that the adsorption process is exothermic in nature and involves a degree of randomness in the arrangement of the adsorbate at the adsorbent interface. The spontaneity of MB adsorption on LP-AC was indicated by a negative value of ΔG Trapped between 0 and − 20 kJ mol^{-1}, indicating that MB adsorption is a physical process. The decreases in ΔG as temperature increases indicated that temperature inhibits the adsorption of MB molecules on LP-AC [66].

Regeneration study

The regeneration of spend activated carbon is an important feature for the economical scale application, that the reuse ability for many cycles enhances its cost effectiveness making it an attractive option for the industrial application. The durability of the produced activated carbon was investigated through the treatment of the spend carbon with 1 M HCl solution followed by subsequent washings with hot distilled water. Adsorption tests were carried using adsorbent mass of 0.045 g in 50 ml of MB solution, then the solution was stirred for 2 h. Fig. S7 (Online Resource 1) demonstrates that LP-AC maintains its performance for four cycles where removal efficiency decreased from 99 to 93%. However, in the fifth cycle removal efficiency decreased to 90%, that could be attributed to the incomplete desorption of dye molecules from the surface which saturate the adsorbent

Table 8 Thermodynamic parameters of MB adsorption

Temperature K	K_d (L g^{-1}) ± SE	ΔH (kJ mol^{-1}) ± SE	ΔS (J mol^{-1} K^{-1}) ± SE	ΔG (kJ mol^{-1}) ± SE
303	18.23 ± 0.023	− 18.50 ± 0.008	36.59 ± 0.005	− 7.41 ± 0.005
313	17 ± 0.014			− 7.04 ± 0.012
323	10.52 ± 0.003			− 6.68 ± 0.003
333	10.26 ± 0.008			− 6.31 ± 0.003

active sites [56]. The applied treatment effectively restores the active sites of the carbon, thereby rendering it reusable multiple times.

Conclusion

Activated carbon derived from low-cost precursor of *L. leucocephala* pods demonstrates high performance in the removal of methylene blue textile dye, achieving a remarkable removal rate of 99.99%. RSM optimization using the Box–Benken design revealed that an initial dye concentration of 300.87 mg L^{-1}, adsorbent dose of 0.049 g, and solution pH of 10.07 are the optimal values that maximize dye removal efficiency. The thermodynamic study showed that the adsorption of MB dye on LP-AC has an exothermic nature with a negative enthalpy. FTIR analysis showed that LP-AC exhibits various surface functional groups such as hydroxyl groups, which enhance the adsorption efficiency of MB. Regeneration study revealed that the prepared carbon exhibits an economic aspect that it could be used for multiple cycles rendering a good performance.

Supplementary Information The online version contains supplementary material available at https://doi.org/10.1007/s11144-024-02677-z.

Funding This research did not receive any specific grant from funding agencies in the public, commercial, or not-for-profit sectors.

Declarations

Conflict of interest The authors declare no competing interests.

References

1. Gohr MS, Abd-Elhamid AI, El-Shanshory AA, Soliman HM (2022) Adsorption of cationic dyes onto chemically modified activated carbon: kinetics and thermodynamic study. J Mol Liq 346:118227. https://doi.org/10.1016/j.molliq.2021.118227
2. Bhatnagar A, Hogland W, Marques M, Sillanpää M (2013) An overview of the modification methods of activated carbon for its water treatment applications. Chem Eng J 219:499–511. https://doi.org/10.1016/j.cej.2012.12.038
3. Zhao W-d, Chen L-P, Jiao Y (2023) Preparation of activated carbon from sunflower straw through H_3PO_4 activation and its application for acid fuchsin dye adsorption. Water Sci Eng 16:192–202. https://doi.org/10.1016/j.wse.2023.02.002
4. Boudghene Stambouli H, Guenfoud F, Benomara A et al (2021) Synthesis of $FeWO_4$ heterogeneous composite by the sol–gel process: enhanced photocatalytic activity on malachite green. Reac Kinet Mech Cat 133:563–578. https://doi.org/10.1007/s11144-021-01994-x
5. Yueqin Yu, Zhao C, Liu X, Sui M, Meng Y (2017) Selective flocculation of pollutants in wastewater using pH responsive HM-alginate/chitosan complexes. J Environ Chem Eng 5:5406–5410. https://doi.org/10.1016/j.jece.2017.10.025
6. Liu H, Zhang J, Lu M et al (2020) Biosynthesis based membrane filtration coupled with iron nanoparticles reduction process in removal of dyes. Chem Eng J 387:124202. https://doi.org/10.1016/j.cej.2020.124202

7. Ikram M, Zahoor M, Batiha GE-S (2021) Biodegradation and decolorization of textile dyes by bacterial strains: a biological approach for wastewater treatment. Z Phys Chem 235:1381–1393. https://doi.org/10.1515/zpch-2020-1708
8. Popovici DR, Neagu M, Dusescu-Vasile CM et al (2021) Adsorption of p-nitrophenol onto activated carbon prepared from fir sawdust: isotherm studies and error analysis. Reac Kinet Mech Cat 133:483–500. https://doi.org/10.1007/s11144-021-01997-8
9. Li X, Tang S, Yuan D et al (2019) Improved degradation of anthraquinone dye by electrochemical activation of PDS. Ecotoxicol Environ Saf 177:77–85. https://doi.org/10.1016/j.ecoenv.2019.04.015
10. Mohamed FF, Allah PM, Mehdi AP, Baseem M (2011) Photoremoval of malachite green (MG) using advanced oxidation process. Res J Chem Environ 15:65–70
11. Surip SN, Abdulhameed AS, Garba ZN et al (2020) H_2SO_4-treated Malaysian low rank coal for methylene blue dye decolourization and cod reduction: optimization of adsorption and mechanism study. Surf Interfaces 21:100641. https://doi.org/10.1016/j.surfin.2020.100641
12. Jawad AH, Mastuli MS, Mallah S, Mastuli S (2019) Adsorption behavior of methylene blue on acid-treated rubber (*Hevea brasiliensis*) leaf. Desalin Water Treat 124:297–307. https://doi.org/10.5004/dwt.2018
13. Xie J, Lin R, Liang Z et al (2021) Effect of cations on the enhanced adsorption of cationic dye in Fe_3O_4-loaded biochar and mechanism. J Environ Chem Eng 9:105744. https://doi.org/10.1016/j.jece.2021.105744
14. Igwegbe CA, Onukwuli OD, Ighalo JO, Okoye PU (2020) Adsorption of cationic dyes on *Dacryodes edulis* seeds activated carbon modified using phosphoric acid and sodium chloride. Environ Process 7:1151–1171. https://doi.org/10.1007/s40710-020-00467-y
15. Luo Y, Li D, Chen Y et al (2019) The performance of phosphoric acid in the preparation of activated carbon-containing phosphorus species from rice husk residue. J Mater Sci 54:5008–5021. https://doi.org/10.1007/s10853-018-03220-x
16. Pang X, Sellaoui L, Franco D et al (2020) Preparation and characterization of a novel mountain soursop seeds powder adsorbent and its application for the removal of crystal violet and methylene blue from aqueous solutions. Chem Eng J 391:123617. https://doi.org/10.1016/j.cej.2019.123617
17. Pathania D, Sharma S, Singh P (2017) Removal of methylene blue by adsorption onto activated carbon developed from *Ficus carica* bast. Arab J Chem 10:S1445–S1451. https://doi.org/10.1016/j.arabjc.2013.04.021
18. Al-Qaim FF, Al-Saedi HFS, Mussa ZH et al (2024) Application of the response surface approach to the adsorption of methylene blue from water using acid-modified grape leaves. Reac Kinet Mech Cat 137:399–422. https://doi.org/10.1007/s11144-023-02542-5
19. Bageel A, Honda MDH, Carrillo JT, Borthakur D (2020) Giant leucaena (*Leucaena leucocephala* subsp. glabrata): a versatile tree-legume for sustainable agroforestry. Agroforest Syst 94:251–268. https://doi.org/10.1007/s10457-019-00392-6
20. Jawad AH, Abdulhameed AS, Mastuli MS (2020) Acid-factionalized biomass material for methylene blue dye removal: a comprehensive adsorption and mechanism study. J Taibah Univ Sci 14:305–313. https://doi.org/10.1080/16583655.2020.1736767
21. Ahmed MJ (2016) Application of agricultural based activated carbons by microwave and conventional activations for basic dye adsorption. J Environ Chem Eng 4:89–99. https://doi.org/10.1016/j.jece.2015.10.027
22. Yahya MA, Al-Qodah Z, Ngah CZ (2015) Agricultural bio-waste materials as potential sustainable precursors used for activated carbon production: a review. Renew Sustain Energy Rev 46:218–235. https://doi.org/10.1016/j.rser.2015.02.051
23. Martínez de Yuso A, Rubio B, Izquierdo MT (2014) Influence of activation atmosphere used in the chemical activation of almond shell on the characteristics and adsorption performance of activated carbons. Fuel Process Technol 119:74–80. https://doi.org/10.1016/j.fuproc.2013.10.024
24. Yusuff AS (2019) Adsorption of hexavalent chromium from aqueous solution by *Leucaena leucocephala* seed pod activated carbon: equilibrium, kinetic and thermodynamic studies. Arab J Basic Appl Sci 26:89–102. https://doi.org/10.1080/25765299.2019.1567656
25. Patidar K, Vashishtha M (2020) Optimization of process variables to prepare mesoporous activated carbon from mustard straw for dye adsorption using response surface methodology. Water Air Soil Pollut 231:526. https://doi.org/10.1007/s11270-020-04893-4
26. Francoeur M, Ferino-Pérez A, Yacou C et al (2021) Activated carbon synthetized from *Sargassum* (sp) for adsorption of caffeine: understanding the adsorption mechanism using molecular modeling. J Environ Chem Eng 9:104795. https://doi.org/10.1016/j.jece.2020.104795

27. Jawad AH, Mohd Firdaus Hum NN, Abdulhameed AS, Mohd Ishak MA (2022) Mesoporous activated carbon from grass waste via H_3PO_4-activation for methylene blue dye removal: modelling, optimisation, and mechanism study. Int J Environ Anal Chem 102:6061–6077. https://doi.org/10.1080/03067319.2020.1807529
28. Oginni O, Singh K, Oporto G et al (2019) Effect of one-step and two-step H_3PO_4 activation on activated carbon characteristics. Biores Technol Rep 8:100307. https://doi.org/10.1016/j.biteb.2019.100307
29. Belhamdi B, Merzougui Z, Laksaci H, Trari M (2019) The removal and adsorption mechanisms of free amino acid L-tryptophan from aqueous solution by biomass-based activated carbon by H_3PO_4 activation: regeneration study. Phys Chem Earth A/B/C 114:102791. https://doi.org/10.1016/j.pce.2019.07.004
30. Li X, Han D, Zhang M et al (2019) Removal of toxic dyes from aqueous solution using new activated carbon materials developed from oil sludge waste. Colloids Surf A 578:123505. https://doi.org/10.1016/j.colsurfa.2019.05.066
31. Solomon D, Kiflie Z, Van Hulle S (2020) Using Box–Behnken experimental design to optimize the degradation of Basic Blue 41 dye by Fenton reaction. Int J Ind Chem 11:43–53. https://doi.org/10.1007/s40090-020-00201-5
32. Sadaf S, Bhatti HN (2016) Response surface methodology approach for optimization of adsorption process for the removal of Indosol Yellow BG dye from aqueous solution by agricultural waste. Desalin Water Treat 57:11773–11781. https://doi.org/10.1080/19443994.2015.1048308
33. Okolo BI, Oke EO, Agu CM et al (2020) Adsorption of lead(II) from aqueous solution using Africa elemi seed, mucuna shell and oyster shell as adsorbents and optimization using Box–Behnken design. Appl Water Sci 10:1–23. https://doi.org/10.1007/s13201-020-01242-y
34. Ahmadi S, Mohammadi L, Rahdar A et al (2020) Acid dye removal from aqueous solution by using neodymium(III) oxide nanoadsorbents. Nanomaterials 10:556. https://doi.org/10.3390/nano10030556
35. Bedada D, Angassa K, Tiruneh A et al (2020) Chromium removal from tannery wastewater through activated carbon produced from *Parthenium hysterophorus* weed. Energ Ecol Environ 5:184–195. https://doi.org/10.1007/s40974-020-00160-8
36. Okpara OG, Ogbeide OM, Ike OC et al (2021) Optimum isotherm by linear and nonlinear regression methods for lead(II) ions adsorption from aqueous solutions using synthesized coconut shell–activated carbon (SCSAC). Toxin Reviews 40:901–914. https://doi.org/10.1080/15569543.2020.1802596
37. Hadi M, Samarghandi MR, McKay G (2010) Equilibrium two-parameter isotherms of acid dyes sorption by activated carbons: study of residual errors. Chem Eng J 160:408–416. https://doi.org/10.1016/j.cej.2010.03.016
38. Manna S, Roy D, Saha P et al (2017) Rapid methylene blue adsorption using modified lignocellulosic materials. Process Saf Environ Prot 107:346–356. https://doi.org/10.1016/j.psep.2017.03.008
39. Mbarki F, Selmi T, Kesraoui A, Seffen M (2022) Low-cost activated carbon preparation from corn stigmata fibers chemically activated using H_3PO_4, $ZnCl_2$ and KOH: study of methylene blue adsorption, stochastic isotherm and fractal kinetic. Ind Crops Prod 178:114546. https://doi.org/10.1016/j.indcrop.2022.114546
40. Raji Y, Nadi A, Mechnou I et al (2023) High adsorption capacities of crystal violet dye by low-cost activated carbon prepared from Moroccan *Moringa oleifera* wastes: characterization, adsorption and mechanism study. Diam Relat Mater 135:109834. https://doi.org/10.1016/j.diamond.2023.109834
41. Fennouh R, Benturki O, Mokhati A et al (2023) Preparation and characterization of highly mesoporous activated carbon from Ziziphus Spina-Christi for tartrazine adsorption from a simulated effluent. Biomass Conv Bioref. https://doi.org/10.1007/s13399-023-04296-5
42. Yilmaz P, Gunduz D, Ozbek B (2021) Utilization of low-cost bio-waste adsorbent for methylene blue dye removal from aqueous solutions and optimization of process variables by response surface methodology approach. Desal Water Treat 224:367–388. https://doi.org/10.5004/dwt.2021.27206
43. Afroze S, Sen TK, Ang M, Nishioka H (2016) Adsorption of methylene blue dye from aqueous solution by novel biomass *Eucalyptus sheathiana* bark: equilibrium, kinetics, thermodynamics and mechanism. Desalin Water Treat 57:5858–5878. https://doi.org/10.1080/19443994.2015.1004115

44. Liu H, Zhang J, Bao N et al (2012) Textural properties and surface chemistry of lotus stalk-derived activated carbons prepared using different phosphorus oxyacids: adsorption of trimethoprim. J Hazard Mater 235:367–375. https://doi.org/10.1016/j.jhazmat.2012.08.015
45. Yorgun S, Yıldız D (2015) Preparation and characterization of activated carbons from Paulownia wood by chemical activation with H_3PO_4. J Taiwan Inst Chem Eng 53:122–131. https://doi.org/10.1016/j.jtice.2015.02.032
46. Nabih MH, El Hajam M, Boulika H et al (2023) Preparation and characterization of activated carbons from cardoon "Cynara Cardunculus" waste: application to the adsorption of synthetic organic dyes. Mater Today 72:3369–3379. https://doi.org/10.1016/j.matpr.2022.07.414
47. Nasrullah A, Saad B, Bhat AH et al (2019) Mangosteen peel waste as a sustainable precursor for high surface area mesoporous activated carbon: characterization and application for methylene blue removal. J Clean Prod 211:1190–1200. https://doi.org/10.1016/j.jclepro.2018.11.094
48. Netto MS, Georgin J, Franco DSP et al (2022) Effective adsorptive removal of atrazine herbicide in river waters by a novel hydrochar derived from *Prunus serrulata* bark. Environ Sci Pollut Res 29:3672–3685. https://doi.org/10.1007/s11356-021-15366-4
49. Koyuncu F, Güzel F, Sayğılı H (2018) Role of optimization parameters in the production of nanoporous carbon from mandarin shells by microwave-assisted chemical activation and utilization as dye adsorbent. Adv Powder Technol 29:2108–2118. https://doi.org/10.1016/j.apt.2018.05.019
50. Chimi T, Hannah BU, Lincold NM et al (2023) Preparation, characterization and application of H_3PO_4-activated carbon from *Pentaclethra macrophylla* pods for the removal of Cr(VI) in aqueous medium. J Iran Chem Soc 20:399–413. https://doi.org/10.1007/s13738-022-02675-9
51. Attallah OA, Mamdouh W (2021) Development and optimization of pectin/chitosan magnetic sponge for efficient cationic dyes removal using Box–Behnken design. Int J Environ Sci Technol 18:131–140. https://doi.org/10.1007/s13762-020-02828-4
52. Afshin S, Rashtbari Y, Vosough M et al (2021) Application of Box–Behnken design for optimizing parameters of hexavalent chromium removal from aqueous solutions using Fe_3O_4 loaded on activated carbon prepared from alga: kinetics and equilibrium study. J Water Process Eng 42:102113. https://doi.org/10.1016/j.jwpe.2021.102113
53. Sahu S, Pahi S, Tripathy S et al (2020) Adsorption of methylene blue on chemically modified lychee seed biochar: dynamic, equilibrium, and thermodynamic study. J Mol Liq 315:113743. https://doi.org/10.1016/j.molliq.2020.113743
54. Sen K, Mondal NK, Chattoraj S, Datta JK (2017) Statistical optimization study of adsorption parameters for the removal of glyphosate on forest soil using the response surface methodology. Environ Earth Sci 76:1–15. https://doi.org/10.1007/s12665-016-6333-7
55. Ahmad NH, Mohamed MA, Yusoff SFM (2020) Improved adsorption performance of rubber-based hydrogel: optimisation through response surface methodology, isotherm, and kinetic studies. J Sol–Gel Sci Technol 94:322–334. https://doi.org/10.1007/s10971-020-05254-7
56. Takele T, Angassa K, Abewaa M et al (2023) Adsorption of methylene blue from textile industrial wastewater using activated carbon developed from H_3PO_4-activated khat stem waste. Biomass Conv Bioref. https://doi.org/10.1007/s13399-023-05245-y
57. Martins AC, Pezoti O, Cazetta AL et al (2015) Removal of tetracycline by NaOH-activated carbon produced from macadamia nut shells: kinetic and equilibrium studies. Chem Eng J 260:291–299. https://doi.org/10.1016/j.cej.2014.09.017
58. Üner O, Geçgel Ü, Bayrak Y (2016) Adsorption of methylene blue by an efficient activated carbon prepared from *Citrullus lanatus* Rind: kinetic, isotherm, thermodynamic, and mechanism analysis. Water Air Soil Pollut 227:247. https://doi.org/10.1007/s11270-016-2949-1
59. Attia AA, Girgis BS, Khedr SA (2003) Capacity of activated carbon derived from pistachio shells by H_3PO_4 in the removal of dyes and phenolics. J Chem Technol Biotechnol 78:611–619. https://doi.org/10.1002/jctb.743
60. Jawad AH, Bardhan M, Islam MA et al (2020) Insights into the modeling, characterization and adsorption performance of mesoporous activated carbon from corn cob residue via microwave-assisted H_3PO_4 activation. Surf Interfaces 21:100688. https://doi.org/10.1016/j.surfin.2020.100688
61. Ibrahim M, Souleiman M, Salloum A (2023) Methylene blue dye adsorption onto activated carbon developed from *Calicotome villosa* via H_3PO_4 activation. Biomass Conv Bioref 13:12763–12776. https://doi.org/10.1007/s13399-021-02027-2
62. Belaissa Y, Saib F, Trari M (2022) Removal of amoxicillin in aqueous solutions by a chemical activated carbons derived from Jujube nuts: adsorption behaviors, kinetic and thermodynamic studies. Reac Kinet Mech Cat 135:1011–1030. https://doi.org/10.1007/s11144-022-02159-0

63. Mozhiarasi V, Natarajan TS (2022) Bael fruit shell-derived activated carbon adsorbent: effect of surface charge of activated carbon and type of pollutants for improved adsorption capacity. Biomass Conv Bioref. https://doi.org/10.1007/s13399-022-03211-8
64. Baytar O, Ceyhan AA, Şahin Ö (2020) Production of activated carbon from *Elaeagnus angustifolia* seeds using H_3PO_4 activator and methylene blue and malachite green adsorption. Int J Phytoremediat. https://doi.org/10.1080/15226514.2020.1849015
65. Daniel LS, Rahman A, Hamushembe MN et al (2023) The production of activated carbon from *Acacia erioloba* seedpods via phosphoric acid activation method for the removal of methylene blue from water. Biores Technol Rep 23:101568. https://doi.org/10.1016/j.biteb.2023.101568
66. Li M, Mu J, Liu Y et al (2023) Removal of phenol by lignin-based activated carbon as an efficient adsorbent for adsorption of phenolic wastewater. Res Chem Intermed 49:2209–2232. https://doi.org/10.1007/s11164-023-04958-z

Authors and Affiliations

Nour El Houda Laouar[1] · Abdelhamid Boukerroui[1] · Chafika Meziti[1,2] · Sylia Azoug[1]

✉ Nour El Houda Laouar
Nourelhouda.laouar@univ-bejaia.dz; nourelhoudalaouar90@gmail.com

[1] Université de Bejaia, Faculté des Sciences Exactes, Laboratoire de Technologie des Matériaux et Génie des Procédés (LTMGP), 06000 Bejaia, Algeria

[2] Faculty of Process Engineering, Salah Boubnider University, Constantine 3, 25000 Constantine, Algeria